A Unified Model for Single/Multifinger HBTs Including Self-Heating Effects

Akhil Garlapati, *Student Member, IEEE,* and Sheila Prasad, *Senior Member, IEEE*

***Abstract*—This paper presents an unified analytical large-signal model that includes self-heating effects. The model is applied to a single-finger AlGaAs/GaAs heterojunction bipolar transistor (HBT) and a multifinger InGaAs/GaAs HBT. The self-heating effect in the HBT is simulated as a feedback from the collector current to the base–emitter voltage. The main advantage of the circuit presented here is that additional analysis of coupling between electrical and thermal circuits is not required, as is the case with the existing models. The small-signal HBT model is implemented based on the S-parameters at multiple frequencies measured at multiple bias points. This model is verified by comparing the measured and simulated S-parameters. The large-signal model is based on the forward Gummel plot and is built over the small-signal model. This model is verified by comparing the simulated and measured dc I–V characteristics.**

***Index Terms*—HBT, model, multifinger, self-heating, single-finger.**

I. Introduction

HETEROJUNCTION bipolar transistors (HBTs) have demonstrated high-power output densities at microwave frequencies and are increasingly being utilized for large-signal applications such as power amplifiers, oscillators, and mixers [1]–[3]. By virtue of their structure, HBTs offer high current handling capability and breakdown voltage, both of which are valuable characteristics for the implementation of power amplifiers [4]. This has been possible because of self-aligned technologies and innovative isolation approaches used to reduce effects of parasitics. These developments lead to the increased use of HBTs in microwave applications such as wireless communications in the 0.8–6-GHz range, high-speed analog and digital circuits, and optoelectronics. The design of these circuits is challenging because of their nonlinear behavior, and accurate large-signal models are required to expedite this process. Hence, for modern computer-aided design (CAD)-based microwave circuit design, there is a need for a unified HBT circuit model that is valid for dc, microwave small-signal, and large-signal operation.

In the case of HBTs, the high power densities associated with these devices can lead to significant operating temperatures when the transistor is used in large-signal applications. Also, since the conductivity of GaAs is very low, self-heating occurs in the device, thereby increasing its temperature. This phenomenon (self-heating) plays a significant role in the prediction of the large-signal behavior of the device. Several approaches that include the self-heating effect in the large-signal model have been reported in the past [5]–[7]. These methods involve a complex analysis of the coupling between the electrical and thermal circuits [8].

This paper presents a simple unified analytical large-signal model, including self-heating effects, applied to single-finger AlGaAs/GaAs and multifinger InGaAs/GaAs HBTs. The model that is presented avoids the complex analysis of the coupling between the electrical and thermal circuits by implementing the self-heating as a feedback from the collector to the base with a current-controlled voltage source. A partial analytical approach is used for the extraction of the small-signal model parameters. The combination of analytical and numerical optimization procedures is exploited to accurately extract the model parameters. The collector current transit time is a very important parameter to be considered when modeling HBTs for microwave and millimeter-wave applications. The collector current transit time is included in the present model as a phase dependence of the base-transport factor. The large-signal model is based on the measured forward Gummel plot and is built over the small-signal model. The overview of this paper is as follows.

Section II presents the small-signal model of the HBT, which is the basis for the large-signal model. Section III presents the large-signal model with an emphasis on the implementation of the self-heating effect. This section highlights the main advantage of the model presented in this paper in comparison with the traditional models. Section IV presents the verification of the model by comparing the simulated and measured characteristics for both the single-finger and multifinger HBTs. This section highlights the fact that a single unified model is used to model both single-finger and multifinger HBTs.

II. Small-Signal Model

The small-signal equivalent circuit of the HBT used in this study is shown in Fig. 1. Although there are many variations of the small-signal equivalent circuit, the intrinsic part of the equivalent circuit is always a T or π topology. The T-type intrinsic equivalent circuit is used in this study since it is more physically meaningful than the circuit with the π topology. The different combinations of the lumped elements added to the intrinsic HBT circuit, as seen in Fig. 1, are used to more accurately characterize the frequency response of the HBTs.

Fig. 2 depicts the physical significance of each of the circuit elements in Fig. 1. The active portion of the HBT is modeled using $C_{\rm be}$, $C_{\rm bc}$, r_e, α, $R_{\rm bc}$, and C_f, where $\alpha = (\alpha_F/1 + jf/f_\alpha)e^{-j\omega\tau}$. α_F is the dc value of transport factor, τ is the

Manuscript received January 19, 2000. This work was supported in part by the National Science Foundation under Grant ECS-9529643.

The authors are with the Department of Electrical and Computer Engineering, Northeastern University, Boston, MA 02115 USA.

Publisher Item Identifier S 0018-9480(01)00022-9.

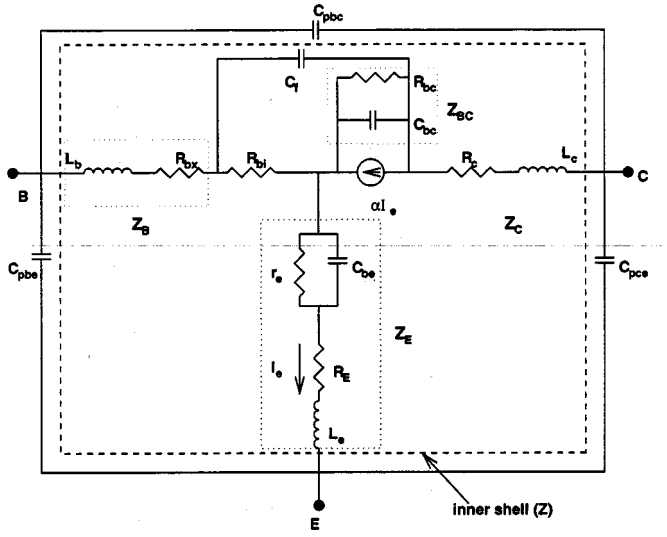

Fig. 1. Equivalent circuit for the small-signal model.

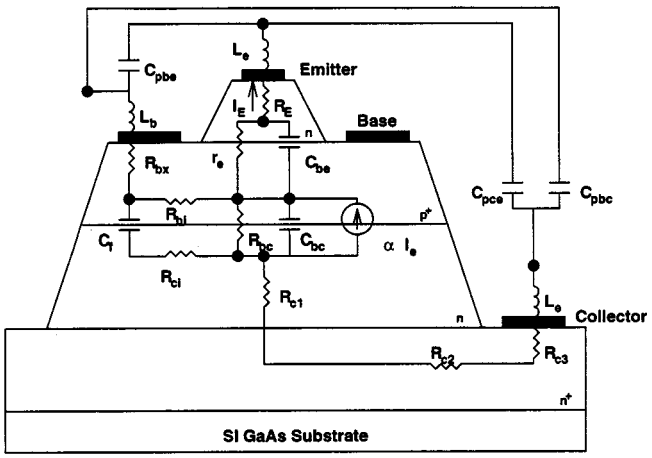

Fig. 2. Physical significance of the small-signal equivalent-circuit elements.

collector current transit time, and f_α is the α 3-dB frequency. The contact resistance and emitter region resistance comprise R_E, the extrinsic emitter resistance. The extrinsic collector resistance is divided into three parts: R_{c1}, R_{c2}, and R_{c3}, due to the n collector, the n^+ access region, and collector contact, respectively. The intrinsic collector resistance is represented by R_{ci}, which characterizes the distributed effect of the base–collector junction at the collector side. Since it is difficult to distinguish between R_{ci}, R_{c1}, R_{c2}, and R_{c3}, and also because the distributed effect at the collector side of the base–collector junction is not as significant as at the base side, all four elements are lumped together as R_c in Fig. 1.

Similarly, the extrinsic base resistance consists of a contact resistance R_{b1} and an access resistance R_{b2}. R_{b1} and R_{b2} are lumped together as R_{bx} in Fig. 1. $R_{\rm bi}$ is the intrinsic base resistance. The distribution effect of the base–collector junction is modeled by the elements $R_{\rm bi}$, R_{bx}, C_f, $C_{\rm bc}$, and $R_{\rm bc}$. $C_{\rm pbe}$, $C_{\rm pbc}$, and $C_{\rm pce}$ model the coupling between the base–emitter, the base–collector, and the collector–emitter interconnection

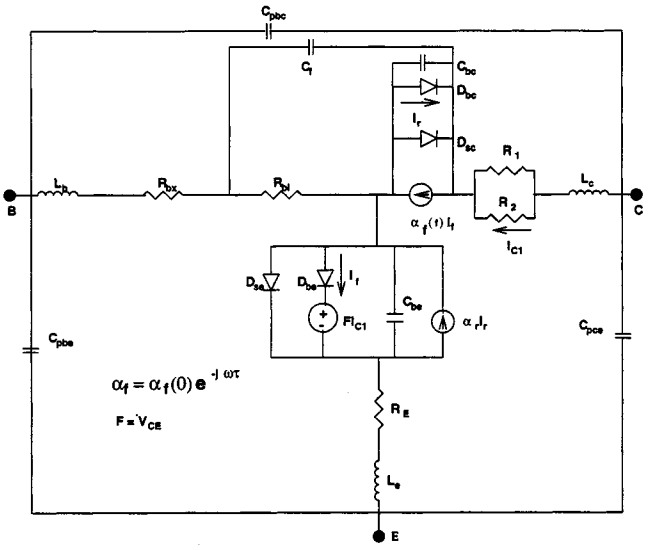

Fig. 3. Schematic of the HBT's large-signal model.

layer. L_e, L_b, and L_c are the contact leads of the emitter, base, and collector, respectively.

All the above-mentioned parameters of the small-signal model are extracted using a partial analytical approach. RF measurements indicate that the HBT under zero bias ($I_b = 0$ A, $V_{CE} = 0$ V) can be represented by a passive network. Therefore, in this case, the transport factor α is negligible. The parasitic elements $C_{\rm pbe}$, $C_{\rm pbc}$, and $C_{\rm pce}$ are evaluated from the reverse-bias scattering-parameter measurements. These parasitics are deembedded from the circuit and the elements of the equivalent circuit, excluding the parasitic effects, are extracted from the resulting Z-parameters. The extrinsic and intrinsic base resistances and the base–collector capacitance are extracted by optimizing the error between the simulated and measured S-parameters.

The elements R_b, L_e, R_e, and R_c are basically constant over the entire frequency range of interest and do not show a significant variation with bias. Therefore, these elements can be considered to be fixed. The bias-dependent elements are C_e, C_{jc}, R_{jc}, α_F, τ, f_α, and r_e. It has been shown that the consideration of the bias variation of these elements is sufficient for accurate small-signal modeling.

III. Large-Signal Model

A modified Ebers–Moll model is used to model the large-signal behavior of the single-finger AlGaAs/GaAs HBT, as well as the multifinger InGaAs/GaAs HBT. The Ebers–Moll model is implemented in the commercial circuit simulator LIBRA. The schematic of the modified Ebers–Moll model for the HBT is shown in Fig. 3. Four diodes are used to model the nonlinearity of the HBT. The variation of forward current gain with the collector current is modeled by the two diodes $D_{\rm be}$ and $D_{\rm se}$. The diode $D_{\rm be}$ represents the electron injection from the emitter, and the diode $D_{\rm se}$ models the neutral base recombination, space–charge region recombination, surface recombination, and the other base leak currents. The two diodes $D_{\rm bc}$

and $D_{\rm sc}$ model the dependence of the reverse current gain on the bias. The diode $D_{\rm bc}$ models the electron injection from the collector to base and the hole injection from the base to the collector. Diode $D_{\rm sc}$ models the neutral base recombination, space–charge region recombination, surface recombination, and the other base leakage currents resulting from the reverse operation. The distributed base–collector junction is modeled by the split base–collector capacitance. The transit time is easily included in the current gain of the Ebers–Moll model.

The effect of the collector transit time τ is included in the base-transport factor α. However, the transit time is a function of the applied bias and it is difficult to implement the bias dependence of τ in the commercial circuit simulator LIBRA. Therefore, the value of the extracted τ at the bias point where the large-signal analysis is carried out is used. Since the bias point is almost in the middle of the load line loci, the extracted value of τ at the bias point should be approximately the average value of τ from the dynamic load line loci. The error in the assumption does not significantly affect the present model as seen from a comparison of the simulated and measured dc characteristics.

The Ebers–Moll model presented in this paper is very similar in form to a previously published extensive large-signal model developed by Grossman and Choma [5]. However, when attempting to implement their model in SPICE, Grossman and Choma had not been able to include the transit time effect in their calculations because of the difficulties involved in working exclusively in the time domain. This problem was circumvented with the Ebers–Moll model in this paper by implementing the transit time delay in the frequency domain. Hence, the delay was simply represented as $e^{-jm\omega_0\tau}$, where m is the harmonic number and ω_0 is the fundamental frequency. The conduction current of the diodes and the displacement current of the nonlinear capacitors are implemented in the time domain, whereas the injection current generators are implemented in the frequency domain. The two domains, i.e., time and frequency, are linked using the LIBRA harmonic-balance software.

The base, collector, and emitter dc currents used to describe the device, which comprise the Ebers–Moll model, are expressed as

$$I_c = \alpha_f I_{\rm be}\left[e^{(qV'_{\rm BE}/n_f kT)}-1\right] - I_{\rm bc}\left[e^{(qV'_{\rm BC}/n_r kT)}-1\right] - I_{\rm sc}\left[e^{(qV'_{\rm BC}/n_{\rm sc} kT)}-1\right] \quad (1)$$

$$I_b = I_{\rm sc}\left[e^{(qV'_{\rm BC}/n_{\rm sc} kT)}-1\right] + I_{\rm se}\left[e^{(qV'_{\rm BE}/n_{\rm sc} kT)}-1\right] + (1-\alpha_r) I_{\rm bc}\left[e^{(qV'_{\rm BE}/n_f kT)}-1\right] \quad (2)$$

$$I_e = I^M_{\rm be}\left[e^{(qV'_{\rm BE}/n_f kT)}-1\right] + I_{\rm se}\left[e^{(qV'_{\rm BE}/n_{\rm sc} kT)}-1\right] - \alpha_r I^M_{\rm bc}\left[e^{(qV'_{\rm BC}/n_r kT)}-1\right] \quad (3)$$

where $V'_{\rm BE}$ and $V'_{\rm BC}$ are the intrinsic base–emitter and base–collector junction voltages, which are calculated as follows:

$$V'_{\rm BE} = V_{\rm BE} - I_e R_E - I_b R_b \quad (4)$$

$$V'_{\rm BC} = V_{\rm BC} - I_c R_c - I_b R_b. \quad (5)$$

TABLE I
EBERS–MOLL MODEL PARAMETERS FOR THE SINGLE-FINGER AlGaAs/GaAs HBT

Component	Value
L_b	46 pH
L_c	87 pH
L_e	20 pH
C_{pbe}	35 fF
C_{pce}	165 fF
C_{pbc}	0 fF
R_b	4 Ω
R_c	4 Ω
R_e	1 Ω
I_{be}	1.429e-23 A
n_f	1.035
M_{je}	0.45
V_{je0}	1.461 V
C_{je0}	131 fF
τ_F	0.74 ps
I_{se}	9.0125e-19 A
n_{se}	1.4812
M_{jc}	0.61
V_{jc0}	1.29 V
C_{jc0}	75 fF
α_F	0.95
f_α	24 GHz

Large-signal parameters are extracted by fitting these equations to the dc measurements. The forward Gummel plot at $V_{\rm BC} = 0$ V is used to extract the current gain β_f, forward saturation current $I_{\rm be}$, the base–emitter leak saturation current $I_{\rm se}$, the forward current ideality coefficient n_f, and the base–emitter leakage emission coefficient $n_{\rm se}$. Since the power dissipation at $V_{\rm BC} = 0$ V is relatively small, the self-heating effect is negligible in the model parameter-extraction procedure.

The device self-heating effect is one of the major concerns in microwave circuit design employing HBTs. Thermal effects in HBTs have been studied using numerical and analytical models by several researchers [6], [7]. Technological solutions that provide thermally stable HBTs have also been addressed [9]. The operating characteristics of an HBT with the self-heating effect can be modeled through the interaction between an electrical and a thermal sub-circuit [10]. A practical feedback circuit, combined with the equivalent Ebers–Moll model of the HBT, is traditionally used to simulate the self-heating effects in the dc characteristics of the devices.

In this paper, a single circuit is used to simulate the large-signal behavior of the HBT including the self-heating effects. The traditional circuit used for the Ebers–Moll model is modified to include the self-heating effects. The modified circuit used in this paper is shown in Fig. 3. The self-heating is implemented as a feedback from the collector current to the base with a current-controlled voltage source. The transfer resistance of the dependent source is a variable equal to the

TABLE II
EBERS–MOLL MODEL PARAMETERS FOR THE MULTIFINGER InGaAs/GaAs HBT

Component	Value
L_b	69 pH
L_c	99 pH
L_e	12 pH
C_{pbe}	80 fF
C_{pce}	71 fF
C_{pbc}	0 fF
R_b	3.5 Ω
R_c	4 Ω
R_e	3 Ω
I_{be}	9.35e-19 A
n_f	1.46
M_{je}	0.46
V_{je0}	0.7 V
C_{je0}	54 fF
τ_F	0.74 ps
I_{se}	6.026e-13 A
n_{se}	3.0
M_{jc}	0.5
V_{jc0}	0.75 V
C_{jc0}	162 fF
α_F	0.983
f_α	25 GHz

applied collector voltage. This feedback reduces the effective base–emitter voltage at high-power consumption, thereby introducing a droop in the collector current, as expected at high temperatures. However, the amount of feedback depends on the thermal resistance of the device, and also on the variation of $V_{\rm BE}$ with base–emitter junction temperature under constant collector current. This is implemented in the model by using the resistances R_1 and R_2. The ratio of these two resistances controls the amount of feedback given from the collector to the base. The ratio of R_1 and R_2 is given by

$$\frac{R_1}{R_2} = \phi R_{\rm th} \tag{6}$$

where ϕ is a factor representing the variation of $V_{\rm BE}$ with base–emitter junction temperature under constant collector current, and has a range of 1–2 mV/K. $R_{\rm th}$ is the thermal resistance of the device. This model has a physical significance in the way it is implemented, which is emphasized in Section IV.

IV. RESULTS AND CONCLUSION

The model presented in this paper is used to simulate single-finger AlGaAs/GaAs and multifinger InGaAs/GaAs HBTs. The multifinger HBT is treated as a single-finger HBT to extract the various elements in the equivalent circuit. This model for the multifinger HBT is valid unless and until the HBT goes into the current collapse region where the base fingers behave differently from one another. This is verified by comparing the simulation results with the measured characteristics.

The extracted small- and large-signal model parameters are given in Table I for the single-finger AlGaAs/GaAs HBT, and in Table II for the multifinger InGaAs/GaAs HBT. The small-signal model is verified by comparing the simulated and measured small-signal S-parameters. From Figs. 4–7, it can be seen

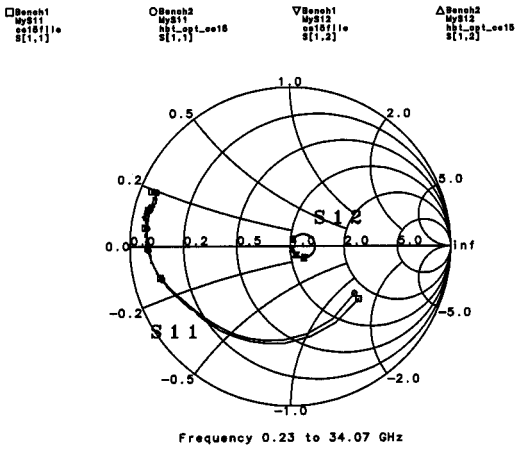

Fig. 4. Simulated and measured S-parameters: single-finger AlGaAs/GaAs HBT.

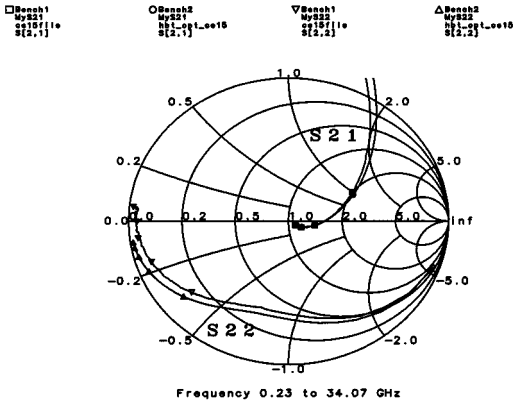

Fig. 5. Simulated and measured S-parameters: single-finger AlGaAs/GaAs HBT.

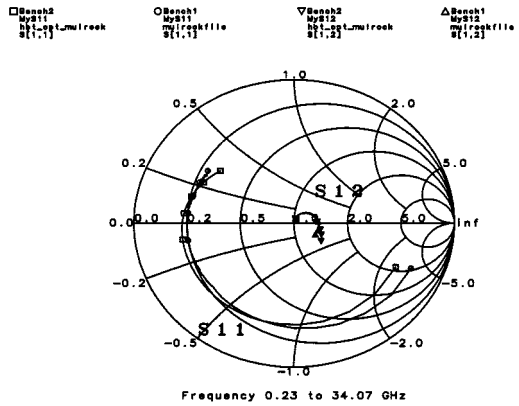

Fig. 6. Simulated and measured S-parameters: multifinger InGaAs/GaAs HBT.

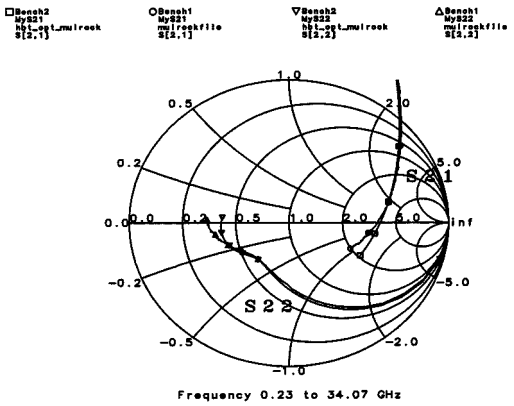

Fig. 7. Simulated and measured S-parameters: multifinger InGaAs/GaAs HBT.

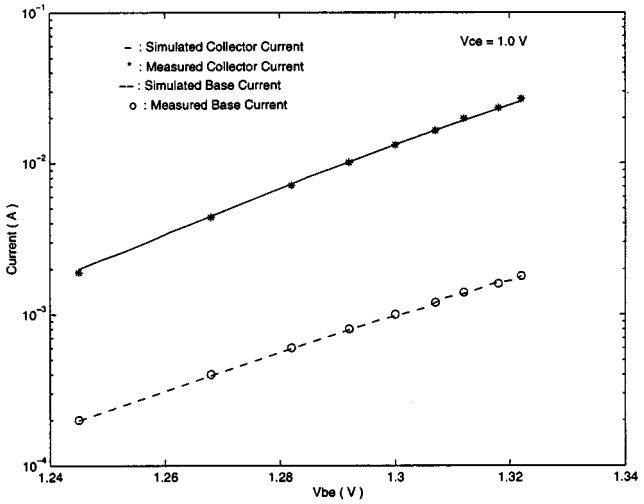

Fig. 8. Gummel plot: single-finger AlGaAs/GaAs HBT.

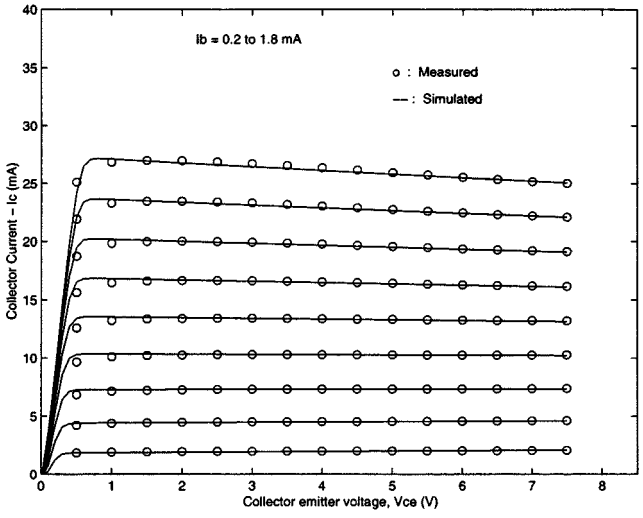

Fig. 9. Simulated and measured dc I–V characteristics: single-finger AlGaAs/GaAs HBT.

that there is a good match between the simulated and measured S-parameters for both the single-finger AlGaAs/GaAs and multifinger InGaAs/GaAs HBTs. The large-signal model is verified by comparing the simulated and measured Gummel

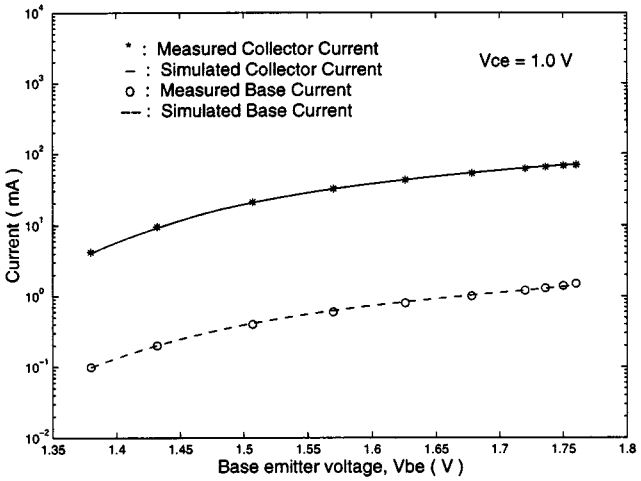

Fig. 10. Gummel plot: multifinger InGaAs/GaAs HBT.

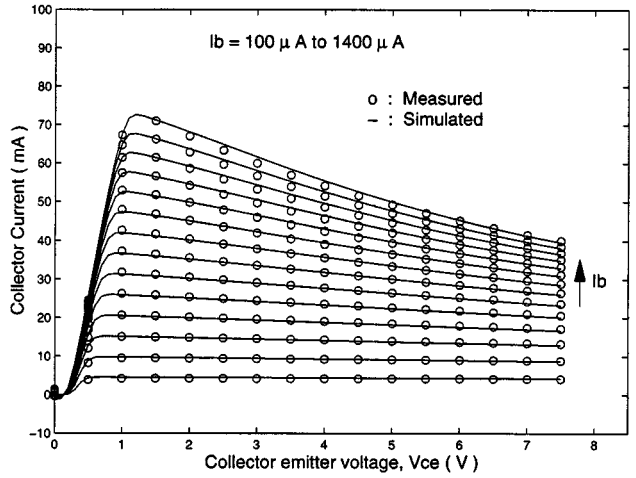

Fig. 11. Simulated and measured dc I–V characteristics: multifinger InGaAs/GaAs HBT.

plots, and the simulated and measured dc I–V characteristics. From Figs. 8–12, it can be seen that there is a good match between the simulated and measured characteristics for both the single-finger AlGaAs/GaAs and multifinger InGaAs/GaAs HBTs.

Fig. 12 depicts the variation of base–emitter voltage $V\mathrm{be}$ with respect to the collector–emitter voltage $V\mathrm{ce}$ for an InGaAs/GaAs multifinger HBT. It can be seen that there is a droop in these characteristics that is similar to the dc I–V characteristics presented in Fig. 11. This leads to the idea that self-heating effects cause a reduction in the base–emitter voltage $V\mathrm{be}$ as the collector–emitter voltage $V\mathrm{ce}$ is increased at high base currents. This reduction in $V\mathrm{be}$ causes the collector current Ic to decrease under high-power operating conditions. The model in this paper is developed from these conclusions. The feedback from the collector current Ic is applied to the base so as to reduce $V\mathrm{be}$ under high-power operating conditions. This shows that the large-signal model presented is valid for single-finger as well as multifinger HBTs.

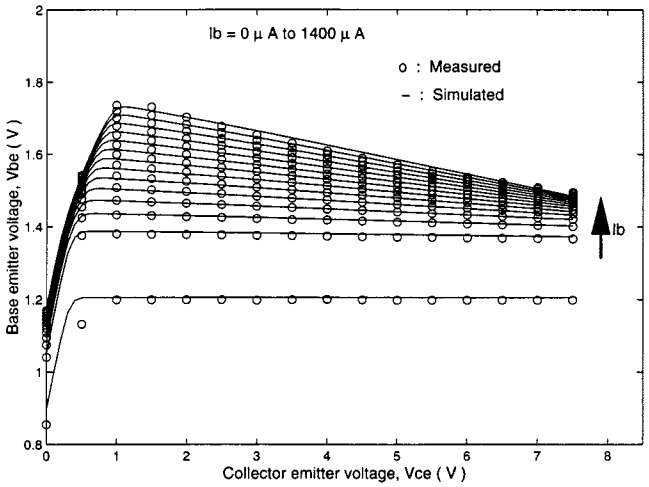

Fig. 12. Simulated and measured characteristics, Vbe versus Vce: multifinger InGaAs/GaAs HBT.

This paper has presented a simple unified analytical large-signal model, including the self-heating effect for an HBT. The model is applied to single-finger and multifinger HBTs and verified by comparing the simulated and measured characteristics. The self-heating effect in the HBT is simulated as a feedback from the collector to the base with a current-controlled voltage source. The main advantage of the circuit presented here is that an additional analysis of the coupling between electrical and thermal circuits is not required as is the case with the existing models. The coupling is built into the circuit itself making the analysis less cumbersome compared to the models proposed previously [8], thereby reducing the convergence problems that arise in the present-day circuit simulations, especially under high-power operating conditions. Both the small- and large-signal models are implemented in the commercial circuit simulator LIBRA and are verified by comparing the simulated and measured small-signal S-parameters and the dc I–V characteristics.

ACKNOWLEDGMENT

The authors wish to thank Prof. C. G. Fonstad, Massachusetts Institute of Technology, Cambridge, for providing the laboratory facilities, Dr. L-W. Yang, TRW Inc., Redondo Beach, CA, for providing the AlGaAs/GaAs HBTs and Rockwell Semiconductor Inc., Thousand Oaks, CA, for providing the InGaAs/GaAs HBTs.

REFERENCES

[1] D. N. McQuiddy, Jr., R. L. Gassner, P. Hull, J. S. Mason, and J. M. Bedinger, "Transmit/receive module technology for X-band active array radar," *Proc. IEEE*, vol. 79, pp. 308–341, Mar. 1991.

[2] P. M. Asbeck, M. C. Chang, J. A. Higgins, N. H. Sheng, G. J. Sullivan, and K. C. Wang, "GaAlAs/GaAs heterojunction bipolar transistor issues and prospects for application," *IEEE Trans. Electron Devices*, vol. ED-36, pp. 2032–2041, Oct. 1989.

[3] M. E. Kim, A. K. Oki, G. M. Gorman, D. K. Umemoto, and J. B. Camou, "GaAs heterojunction bipolar transistor device and IC technology for high-performance analog and microwave application," *IEEE Trans. Microwave Theory Tech.*, vol. 37, pp. 1286–1303, Sept. 1989.

[4] G. B. Gao, H. Morkoc, and M. C. Chang, "Heterojunction bipolar transistor design for power applications," *IEEE Trans. Electron Devices*, vol. 39, pp. 1987–1997, Sept. 1992.

[5] P. C. Grossman and J. Choma, "Large signal modeling of HBT's including self-heating and transit time effects," *IEEE Trans. Microwave Theory Tech.*, vol. 40, pp. 449–464, Mar. 1992.

[6] L. L. Liou and J. L. Ebel, "Thermal effects on the characteristic of AlGaAs/GaAs heterojunction bipolar transistor using two-dimensional numerical simulation," *IEEE Trans. Electron Devices*, vol. 40, pp. 35–43, Jan. 1993.

[7] L. L. Liou, B. Bayraktaroglu, and C. I. Huang, "Theoretical thermal runaway analysis of heterojunction bipolar transistors: Junction temperature rise threshold," *Solid State Electron.*, vol. 39, pp. 165–172, 1996.

[8] B. Li, S. Prasad, L. W. Yang, and S. C. Wang, "Large signal characterization of AlGaAs/GaAs HBTs," *IEEE Trans. Microwave Theory Tech.*, vol. 47, pp. 1743–1746, Sept. 1999.

[9] B. Bayraktaroglou, J. Barrette, L. Kehias, C. I. Huang, R. Fitch, and R. Scherer, "Very high-power-density CW operation of GaAs/AlGaAs microwave heterojunction bipolar transistors," *IEEE Electron Device Lett.*, vol. 14, pp. 493–495, Oct. 1993.

[10] K. Wu and P. A. Perry, "A new large-signal AlGaAs/GaAs HBT model including self-heating effects, with corresponding parameter-extraction procedure," *IEEE Trans. Microwave Theory Tech.*, vol. 43, pp. 1433–1445, July 1995.

Akhil Garlapati (S'97) was born on September 3, 1975, in Hyderabad, India. He received the B.Tech degree in electrical engineering from the Indian Institute of Technology, Madras, India, in 1997, the M.S. degree in electrical engineering from Northeastern University, Boston, MA, in 1999, and is currently working toward the Ph.D. degree at Northeastern University.

During the summer of 1999, he was with Analog Devices, where he was involved with the development of HBT models. His research interests include characterization and modeling of HBTs for microwave applications and RF circuit design.

Sheila Prasad (SM'82) received the B.Sc. degree from the University of Mysore, Bangalore, India, and the S.M. and Ph.D. degrees in applied physics from Harvard University, Cambridge, M.A.

She has been on the faculty of the Department of Electrical Engineering, New Mexico State University, Las Cruces, NM, and the Department of Electrical and Electronics Engineering, Birla Institute Technology of Science, Pilani, India. She has also been a Visiting Professor of applied physics at the American University, Cairo, Egypt, a Visiting Senior Scientist at the Indian Institute of Science, Bangalore, India, and a Visiting Scientist at the Center for Materials Science and Engineering, Massachusetts Institute of Technology, Cambridge. She is currently a Professor in the Department of Electrical and Computer Engineering, Northeastern University, Boston, MA. Her research interests include microwave and high-speed semiconductor devices, microwave solid-state circuits, and optoelectronic devices and circuits. She has authored or co-authored numerous journal papers and international conference presentations on the high-frequency characterization and modeling of devices and circuits, and has also developed applications of the simulated annealing algorithm and neural networks. She also co-authored *Fundamental Electromagnetic Theory and Applications* (Englewood Cliffs, NJ: Prentice-Hall, 1986). She is a Reviewer for a variety of journals.

Dr. Prasad is a member of is Sigma Xi. She is an Editorial Board member for the IEEE TRANSACTIONS ON MICROWAVE THEORY AND TECHNIQUES.